minerals

MDPI

Article

Episodic Fluid Action in Chinese Southwestern Tianshan HP/UHP Metamorphic Belt: Evidence from U–Pb Dating of Zircon in Vein and Host Eclogite

Zhen-Yu Chen [1,*], Li-Fei Zhang [2], Zeng Lü [2] and Jin-Xue Du [3]

[1] MNR Key Laboratory of Metallogeny and Mineral Assessment, Institute of Mineral Resources, Chinese Academy of Geological Sciences, Beijing 100037, China
[2] MOE Key Laboratory of Orogenic Belts and Crustal Evolution, School of Earth and Space Sciences, Peking University, Beijing 100871, China; lfzhang@pku.edu.cn (L.-F.Z.); luzeng@pku.edu.cn (Z.L.)
[3] School of Earth Sciences and Resources, China University of Geosciences, Beijing 100083, China; dujinxue1@163.com
* Correspondence: czy7803@126.com

Received: 11 October 2019; Accepted: 21 November 2019; Published: 25 November 2019

Abstract: Fluid plays a key role in metamorphism and magmatism in subduction zones. Veins in high-pressure (HP) to ultrahigh-pressure (UHP) rocks are the products of fluid–rock interactions and can thus provide important constraints on fluid processes in subduction zones. In this study, we present an integrated study of zircon in situ U–Pb dating, trace element and mineral inclusion analysis for a complex vein and its host eclogite in the southwestern Tianshan UHP terrane, aiming to decipher the episodic fluid action during slab subduction and exhumation. Both zircon in eclogite and vein have euhedral, prismatic morphology similar to those crystallized from metamorphic fluid. Zircon in eclogite shows core–rim structures with distinct bounds and mineral inclusions. Zircon in the vein shows sector zoning or weak zoning, with bright rims around most zircon grains, which suggests recrystallization of the zircon crystals after their formation and multiple evolution of the vein. Eclogite zircon rims yield a weighted mean of 311 ± 3 Ma and cores yield a range from 413 ± 4 to 2326 ± 18 Ma, respectively. Vein zircon yields four groups of age (~355 Ma, ~337 Ma, ~315 Ma, and ~283 Ma), which date four episodes of fluid flow involving zircon growth. The first two groups of age may represent prograde epidote–amphibolite facies and amphibolite/blueschist facies metamorphism stage, respectively. The third group is similar to that of eclogite zircon rims, which is thought to date the eclogitic facie metamorphism (320–305 Ma), and the fourth group dates a later retrograde metamorphism after greenschist facies. The vein-forming fluid system was supposed to be an open system indicated by trace element of vein zircon and mineral assemblage of the vein. The coexistence of rutile, zircon, and garnet in prograde vein and the heavy rare earth elements (HREE) enrichment characteristic of vein zircon suggest that the vein-forming fluid are enriched in high field strength elements (HFSE) and HREE, and such fluid could be formed under low P–T conditions.

Keywords: zircon; vein; eclogite; U–Pb dating; trace elements; southwestern Tianshan

1. Introduction

In subduction zone metamorphism, fluid plays a key role in many geological processes including metasomatism, crustal rheology, anatexis, resetting of isotopic clocks, transformation of mineral assemblages, and formation and preservation of high-pressure (HP) and ultrahigh-pressure (UHP) rocks [1–7]. Veins are common in subduction zone metamorphic rocks and they are considered products of mineral precipitation from metamorphic fluid. As such, they provide vital information for fluid processes in subduction zones [8–12].

Many studies have been conducted on various veins within HP–UHP metabasites in oceanic subduction zones [8,10,11,13,14]. These studies unraveled that, on the one hand, veining primarily occurred at prograde transformation from blueschist facies to eclogite facies during subduction. On the other hand, different stages of veining may occur in the same HP to UHP metamorphic slices, suggesting that the origin of vein-forming fluids is complicated, and both internal and external fluids may be involved in veining [11,15–17]. Nevertheless, retrograde hydration during exhumation of the subducted oceanic crust is also notable, triggering the back transformation of eclogite into blueschist [16,18] and formation of HP veins in eclogite [19,20].

In high-grade metamorphic rocks, fluid availability plays a critical role in dictating zircon growth or overgrowth [21–24], and zircon always has complex multiple growth textures and can serve as the best mineral to preserve the metamorphic evolution [25]. Many previous studies have shown that metamorphic zircon can be formed in veins (quartz vein or complex vein) related to eclogite, and vein zircon can be formed during the prograde, peak, and retrograde stages. Together with zircon in wall-rock eclogite, metamorphic and vein zircon can record the whole evolution history of eclogite with protolith, prograde, peak, and retrograde ages, as well as reflect the timing of fluid actions [14,21,26–31]. On the other hand, trace elements of zircon in the vein can provide information on the properties of the vein-forming fluid [28–31].

There are plenty of veins in eclogite and blueschist from southwestern Tianshan. Some of these veins are thought to be formed during prograde stage [11,32], and some are considered to be formed during retrogressive stage [16,18–20]. However, the time of vein forming, and thus the fluid action, has not been constrained definitely to date. In this paper, we conducted in situ U–Pb dating, trace element analysis, and mineral inclusion analysis on zircons in a vein and its host eclogite from southwestern Tianshan. The results added new constraint on the timing of eclogite and, more importantly, gave constraint on episodic timing and provenance of fluid flow during subduction and exhumation of oceanic crust.

2. Geological Setting and Sample Descriptions

The blueschist–eclogite belt in southwestern Tianshan is located between the Yili-Central Tianshan and Tarim plates along the South Central Tianshan suture and is assumed to be formed as a result of tectonic amalgamation between the Yili-Central Tianshan and Tarim plates [33–35]. It extends approximately 200 km in length in Xingjiang, northwest China and is mainly distributed in Zhaosu County (Figure 1). It is bounded by two ductile shear zones. To the north, it is separated from the low pressure/high temperature (LP/HT) metamorphic belt consisting of cordierite-bearing garnet–sillimanite gneiss and two-pyroxene granulite [35], and to the south, from the unit of interlayered marble and chlorite–white mica schist [36]. This belt consists of eclogite, blueschist, phengite schist, and greenschist, and is associated with serpentinized ultramafic rocks [37–39]. Eclogite and blueschist mainly occur as lens or blocks in widespread garnet-mica schists. Geochemical studies have suggested that the protoliths of these HP–UHP metabasic rocks are of oceanic affinity [16,40,41]. Well-preserved coesite inclusions were discovered in eclogitic rocks from the Habutengsu–Kebuerte unit (HKU) recently (Figure 1, [42–46]), which confirmed that the protoliths of these schists and eclogites undoubtedly experienced UHP metamorphism [47–50]. The peak P–T condition of eclogitic rocks mainly ranged from 500–600 °C at 2.0–3.0 GPa [20,37,38,42–44,51–53]. More data has suggested that the age of UHP metamorphism in the southwestern Tianshan were Late Paleozoic [54–60].

Veins are ubiquitous and occur as networks in eclogites and blueschists on scales of centimeter to meter. They are predominantly composed of omphacite, quartz, epidote, amphibole, carbonate, garnet, and rutile in variable modal proportions [11,19,61]. Some veins were interpreted as a result of the dehydration of blueschist during prograde metamorphism [11,16,32,61]. However, retrograde hydration was also found to trigger the back transformation of eclogite into blueschist [18], and some veins were thought to be formed at the stage of retrograde epidote–amphibolite facies [20] or retrograde eclogite facies [16,62] by lawsonite dehydration during the exhumation of the subducted oceanic crust.

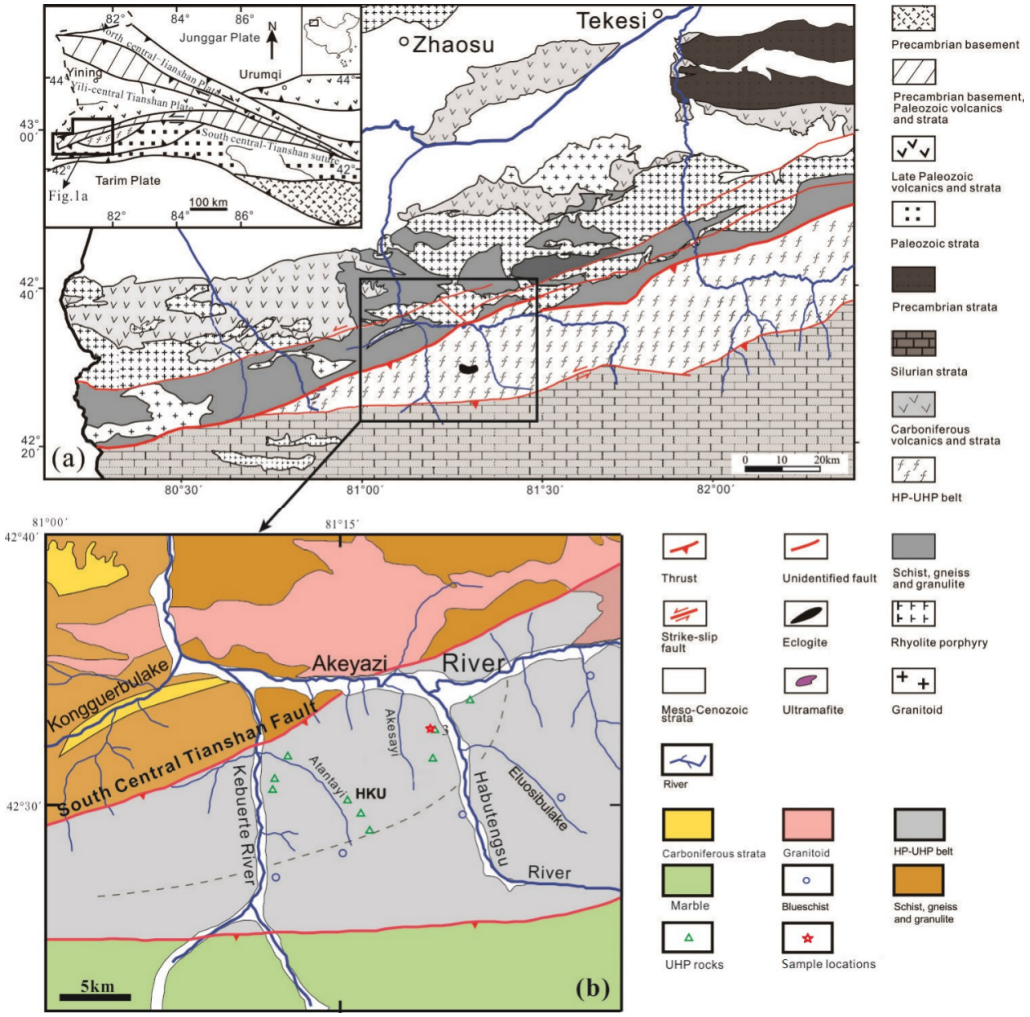

Figure 1. (**a**) Geological sketch map of the southwestern Tianshan orogenic belt in northwest China; (**b**) Geological sketch map of the Habutengsu–Kebuerte low temperature/ultrahigh-pressure (LT/UHP) eclogite facies unit (HKU) with sample localities. The dashed line represents the possible boundary of HKU [63]. The locations of UHP rocks are from [19,42–46]. Maps are modified after [19,62].

The eclogite and vein in this study were sampled from the Habutengsu area and were intimately associated with coesite-bearing rocks [42–45]. The eclogite sample (H11-5) was made of lens-shaped eclogites surrounded by pelitic–felsic schist, mainly composed of garnet, omphacite, paragonite, glaucophane, and barroisite, as well as minor amounts of quartz, rutile, and zircon (Figure 2A). Garnet was euhedral and porphyroblastic in the studied sample and omphacite occurred as fibrous, elongated, or patchy aggregate in the matrix. The modal abundance of mineral assemblage was about 30% garnet, 50% omphacite, 5% paragonite, 8% glaucophane and barroisite, 5% quartz, and 2% other minerals.

The vein sample (H10-3) cross-cut blueschist and eclogite in the same sampling point of H11-5. Compared with fine-grained host eclogites, the veins distinctly contained very low modal amounts of garnet and clinopyroxene (<5%), and displayed large crystals of epidote (clinozoisite), carbonate, quartz, white mica, rutile, and sphene, with accessory zircon and apatite (Figure 2B). Garnet shows euhedral zoning, which is 100–500 μm in size. Clinopyroxene occurs as elongated grain with some hornblende as alteration product. Clinozoisite occurs as a long thread-like structure of cellulose, varying from 0.5 mm to 3 mm in width and 5 mm to 15 mm in length, with modal abundance of about 30%. Carbonate is predominantly ankerite and dolomite with modal abundance of about 20%. White mica occurs as large flakes and fine-grained aggregates, and tends to be gartered in the contact site with eclogite, with modal abundance of about 10%. Both rutile and sphene have two occurrences:

One as primary coarse grains with small alteration rims (Figure 3A), and other as secondary irregular grains associated with small grains of clinozoisite, hornblende, and quartz. During sampling of the vein, any parts containing eclogite were discarded to avoid contamination.

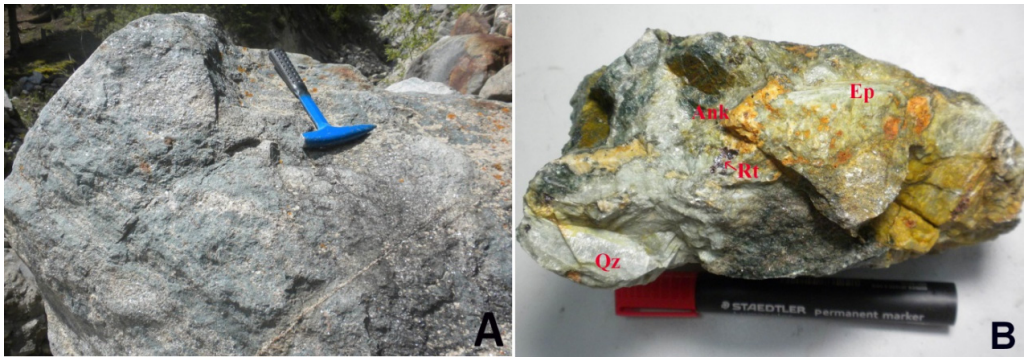

Figure 2. Field photographs and photomicrographs of the eclogite and vein sample from the Habutengsu area, the southwestern Tianshan Orogen. (**A**) Field photographs of eclogite sample H11-5. (**B**) Photographs of vein sample H10-3. Ank—ankerite; Ep—epidote; Qz—quartz; Rt-rutile.

3. Analytical Methods

Major element compositions of the minerals in the vein and mineral inclusions in zircon were determined on a JEOL-8230 electron microprobe (EMP) at the Institute of Mineral Resources, Chinese Academy of Geological Sciences (CAGS). The working conditions were at 15 kV of accelerating voltage, 20 nA of beam current, and 1–5 μm of beam diameter. Natural minerals and synthetic oxides were used as standards, and a program based on the ZAF procedure was used for data correction. The error for all elements was below 5%.

Zircon grains were extracted from about 2 kg of the vein and 5 kg of the eclogite by crushing, sieving, and standard heavy-liquid and magnetic separation techniques. Zircon grains selected by examination with a binocular microscope were mounted in epoxy resin, polished to approximately half thickness, and imaged with a cathodoluminescence (CL) detector in the same electron microprobe as was mentioned above. The operating conditions for the CL imaging were 20 kV and 8 nA. Cathodoluminescence (CL) images were obtained to characterize each grain in terms of size, growth morphology, and internal structure, and were used to guide analytical spot selection for U–Pb dating and trace-element analysis.

U–Pb dating and trace element analyses of zircon in the vein and eclogite were conducted synchronously by (Laser Ablation-Inductively Coupled Plasma-Mass Spectrometer) LA-ICP-MS at the State Key Laboratory of Geological Processes and Mineral Resources, China University of Geosciences, Wuhan. Detailed operating conditions for the laser ablation system and the ICP-MS instrument and data reduction were previously described by [64–66]. During the elemental and isotopic analyses of zircons, the time-resolved LA-ICP-MS count diagrams were monitored to avoid any submicroscopic inclusions. Analysis spots which showed abnormal Si, Al, Ti, Ca, or other elements, demonstrating the involvement of silicate, rutile, apatite, or other inclusions, were abandoned or excluded from the further discussion.

4. Results

4.1. Mineral Chemistry of the Vein

Since the eclogite in the nearly same location has been studied by [43] in detail, we only analyzed the minerals in vein sample H10-3. Garnet in the vein showed obvious growth zoning, with CaO and MgO content increasing from the core to rim, and FeO, MnO content decreasing from the core to rim (Table S1, Figure 3B), which suggested a prograde growth with increasing pressure and temperature.

Clinopyroxenes in vein fell in the compositional field of omphacite, and compositional zoning was not detected across vein omphacite. White micas in the vein were paragonite with no composition zoning. Clinozoisites in the vein were characterized by the values of $Fe^{3+}/(Fe^{3+} + Al)$ of about 0.05. The vein sphene contained 2.67 wt.% Al_2O_3 (Table S1). Apatite in the vein displayed an average F content of 2.67 wt.% and Cl content of 0.17% (Table S2).

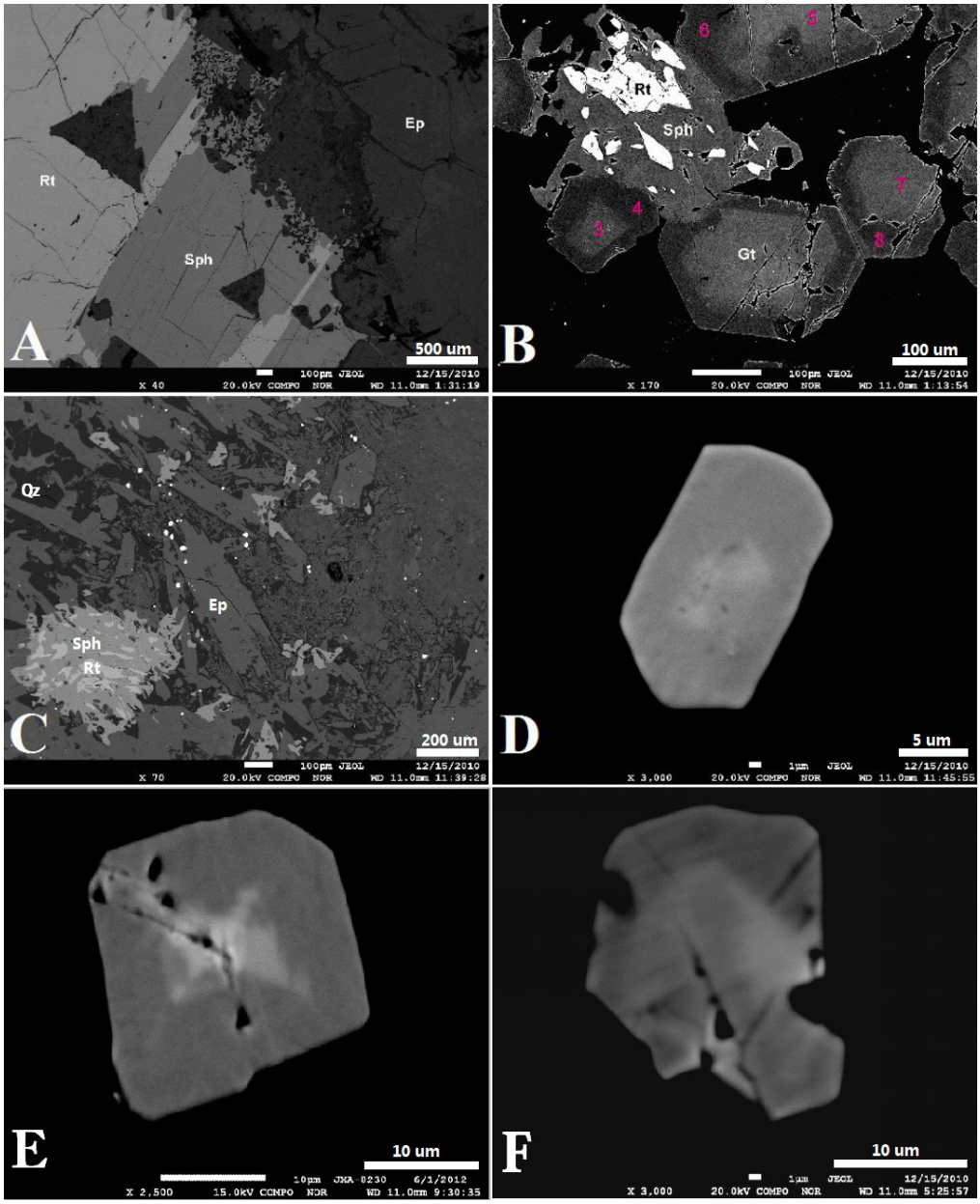

Figure 3. Backscatter electron (BSE) images of vein sample H10-3. (**A**) Vein sample contain epidote, rutile, and sphene as major minerals; (**B**) garnet in vein show obvious prograde growth zoning, numbers on garnet represent the EMP analyze spots corresponding to the numbers in Table S1; (**C**) many tiny zircons (brightest dot in the BSE image) can be found in the thin section of vein sample; (**D**–**F**) amplified images of some of the tiny zircons found in the thin section of vein sample. Ep—epidote; Gt—garnet; Qz—quartz; Rt—rutile; Sph—sphene.

Many tiny zircons were found in the thin section of vein sample (Figure 3C–F). Most of these tiny zircons were less than 30 μm in length and showed euhedral, short prisms in backscatter electron (BSE) images with a brighter core and darker rim. Since there was a negative correlation in brightness

between the CL and the BSE images of the same zircon domain [67], these tiny zircons were very similar to the morphology and internal structure of zircon grains extracted from the vein (see the next section), suggesting a new growth origin of these zircons.

4.2. Zircon Morphology and Mineral Inclusions

Zircon grains extracted from eclogite were euhedral, short to long prismatic, light-yellow to colorless, and transparent. Their lengths ranged from 50 μm to 150 μm, with aspect ratios of 2:1 to 4:1. In the CL images (Figure 4), the zircon grains showed core–rim structures with distinct bounds between the core and rim. The cores were about 20–80 μm in size and often had an incomplete crystal shape or an embayed outline. The inner structure of cores varied significantly. Some showed obvious oscillatory zoning, while some showed sector zoning or weak zoning. These observations indicate that the cores were either igneous zircon from protolith or inherited detrital zircon with complex sources. The rims showed weak oscillatory zoning and were sometimes surrounded by a high-luminescent outer rim (Figure 4). This core–rim structure and inner structure of core and rim were very similar to zircon in the jadeite–quartz vein within eclogite from the Sesia–Lanzo Zone of west Alps reported by [21], and were also similar to zircon in a quartz vein within eclogite from the Dabie orogen [30]. The zoning pattern of rims was also similar to the zircon crystallized in metamorphosed veins [14,26], suggesting these rims were crystallized in fluid-rich conditions. The core and rim had distinct mineral inclusions. Index high-pressure metamorphic mineral inclusions such as rutile, omphacite, and phengite were found in rims, and quartz, albite, and apatite were found in the cores (Figure 5, Table S3).

Zircon grains extracted from vein were euhedral, short-prismatic, colorless, and transparent. Most of grains were less than 100 μm in length and several exceeded 200 μm, with aspect ratios of less than 2:1. In the CL images (Figure 6), the zircon grains showed sector zoning or weak zoning, which is common in crystallized metamorphic hydrothermal zircon [12,14,21,26,27]. CL-bright rims were observed around most zircon grains, which may represent recrystallization of the zircon crystals after their formation [23]. This, in turn, may suggest multiple evolution of the vein [27]. Rutile, omphacite, epidote, actinolite, paragonite, titanite, and chlorite were found as mineral inclusions in these zircons by EMP analysis (Figure 7, Table S3).

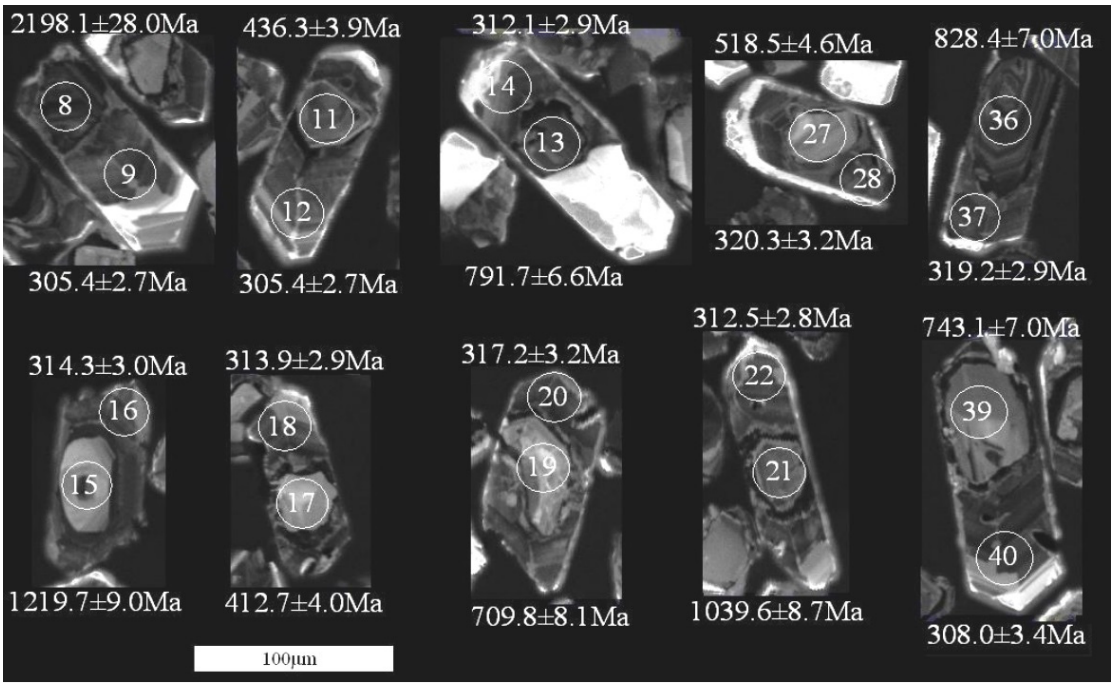

Figure 4. Typical cathodoluminescence (CL) images of zircon in eclogite (the number in circle denote the LA-ICP-MS dating spot, the corresponding ages are showed near the circle).

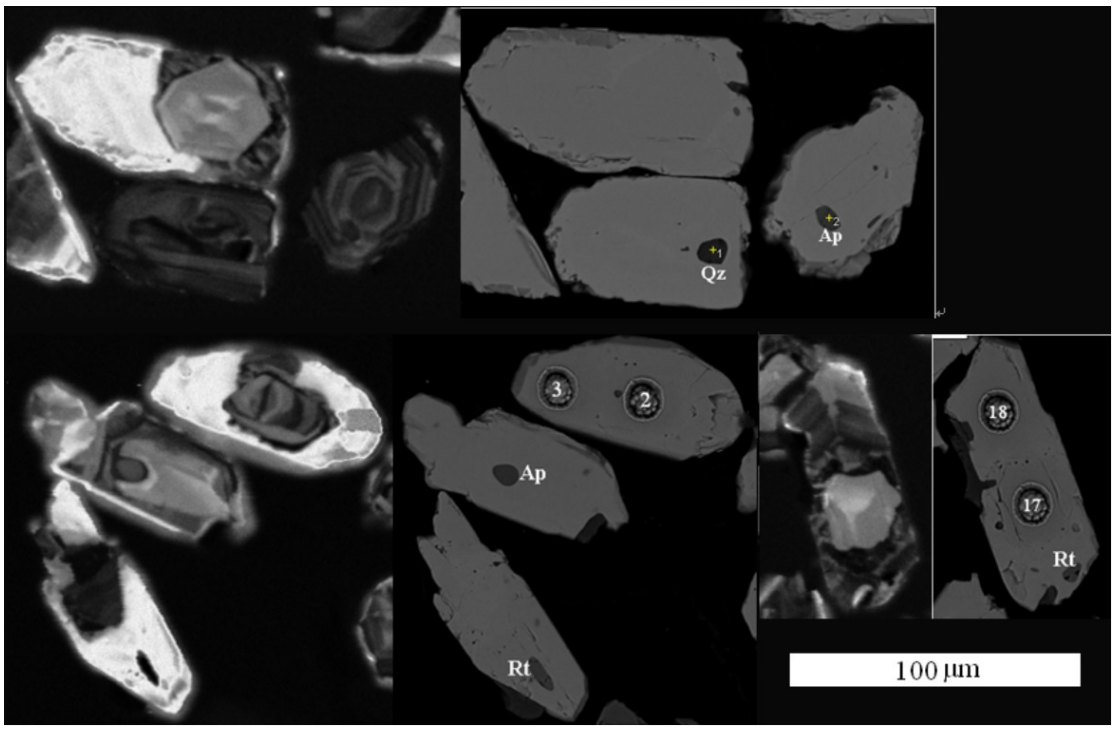

Figure 5. Typical CL and BSE images show inner structure and mineral inclusions in zircon from eclogite H11-5. The pit and number denote the LA-ICP-MS dating spot. Ap—apatite; Qz—quartz; Rt—rutile.

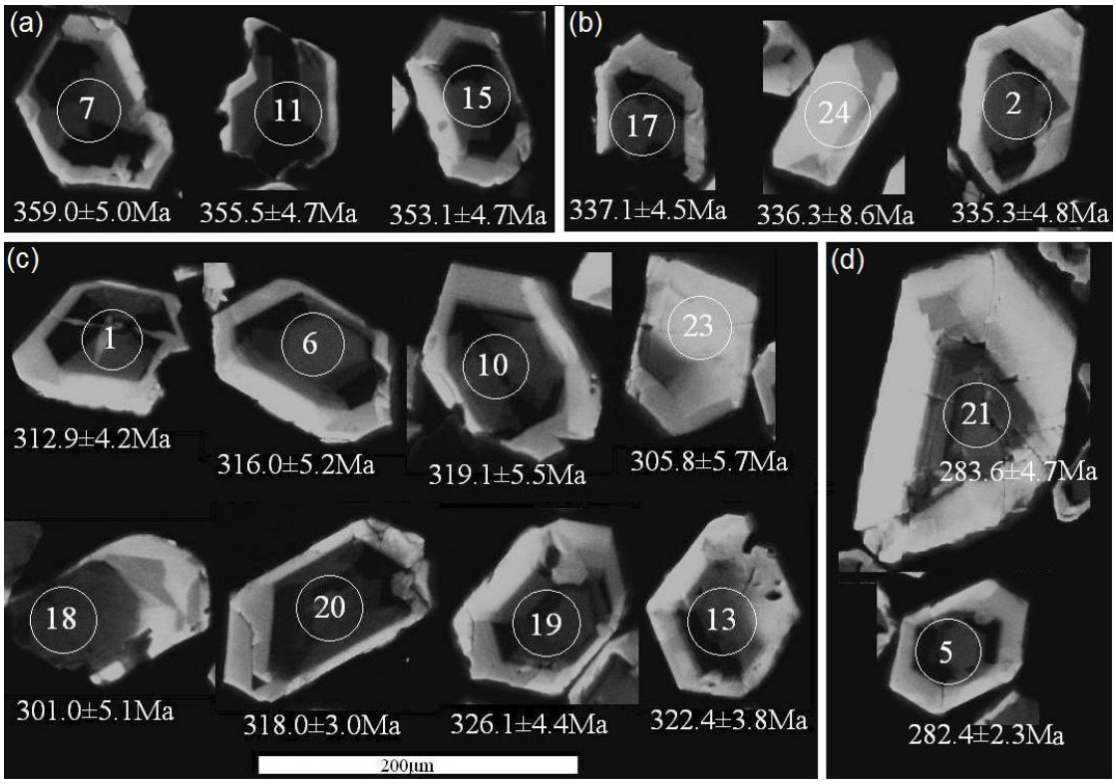

Figure 6. Typical CL images of zircon in vein H10-3 with LA-ICP-MS dating spot and corresponding ages. (**a**)–(**d**) represent four age groups of zircons, respectively. Note that Group IV zircon had many fractures (**d**).

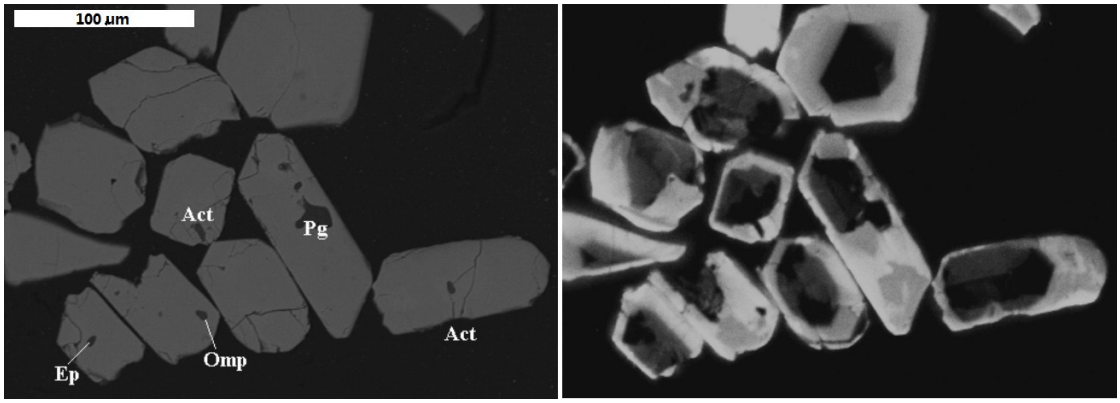

Figure 7. Typical CL and BSE images show inner structure and mineral inclusions in zircon from vein H10-3. Act—actinolite; Ep—epidote; Omp—omphacite; Pg—paragonite.

4.3. Zircon U–Pb Ages

Forty analyses of zircons in eclogite H11-5 are reported in Table S4. Eighteen spots on zircon rims yield protracted concordant $^{206}Pb/^{238}U$ apparent ages ranging from 301 ± 3 to 320 ± 3 Ma, with a weighted mean age of 311 ± 3 Ma (2σ, MSWD = 3.8, Figure 8). The rims had very low Th content of less than 1.46 ppm, U contents ranging from 16 ppm to 300 ppm, and low Th/U ratios of ≤ 0.019, similar to hydrothermal origin zircon [12,14,27,68]. Seventeen spots on zircon cores yielded concordant $^{206}Pb/^{238}U$ apparent ages ranging from 413 ± 4 Ma to 2326 ± 18 Ma, with Th/U ratios of 0.302 to 1.666. The other five spots yielded discordant ages. These spots were all on the high-luminescent rims. The discordant ages could be caused by very low Th (some of them less than detection limit of LA-ICP-MS) and U content (<5 ppm).

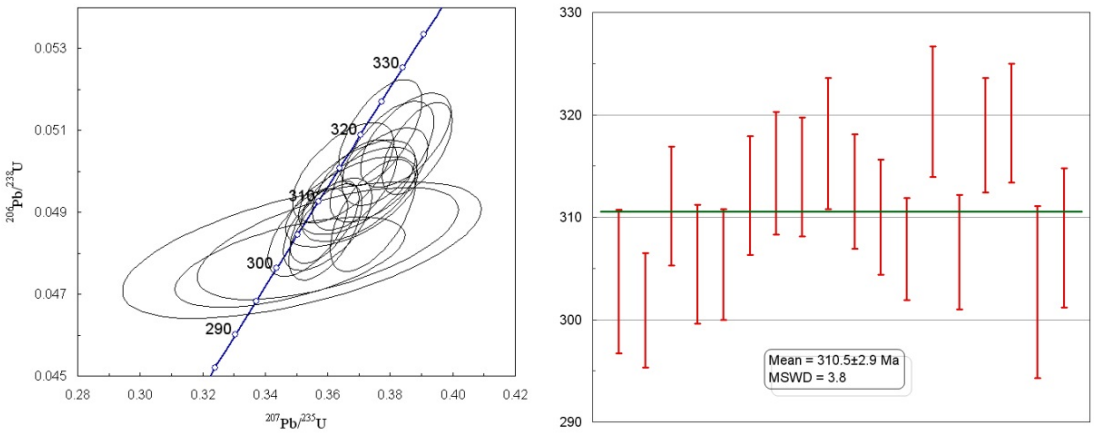

Figure 8. Concordia and weighted mean diagrams for U–Pb ages of zircon rims in eclogite H11-5. Error ellipses are shown at 1 σ. Weighted mean at 2 σ.

Thirty analyses of zircons in vein H10-3 are reported in Table S5. The ages can be divided into four groups. Group I: Five spots yielded $^{206}Pb/^{238}U$ apparent ages ranging from 353 ± 13 to 359 ± 5 Ma, with a weighted mean age of 355 ± 5 Ma. Group II: Seven spots yield $^{206}Pb/^{238}U$ apparent ages ranging from 332 ± 3 Ma to 341 ± 4 Ma, with a weighted mean age of 337 ± 3 Ma. Group III: Fifteen spots yield $^{206}Pb/^{238}U$ apparent ages ranging from 300 ± 4 to 326 ± 4 Ma, with a weighted mean age of 315 ± 4 Ma. Group IV: Three spots yield $^{206}Pb/^{238}U$ apparent ages ranging from 282 ± 4 to 284 ± 5 Ma, with a weighted mean age of 283 ± 5 Ma (Figure 9). The four groups had Th/U ratios ranging in 0.003–0.014, and most of them had Th content lower than 3 ppm. Zircons of these four groups showed similar inner structures to their CL images.

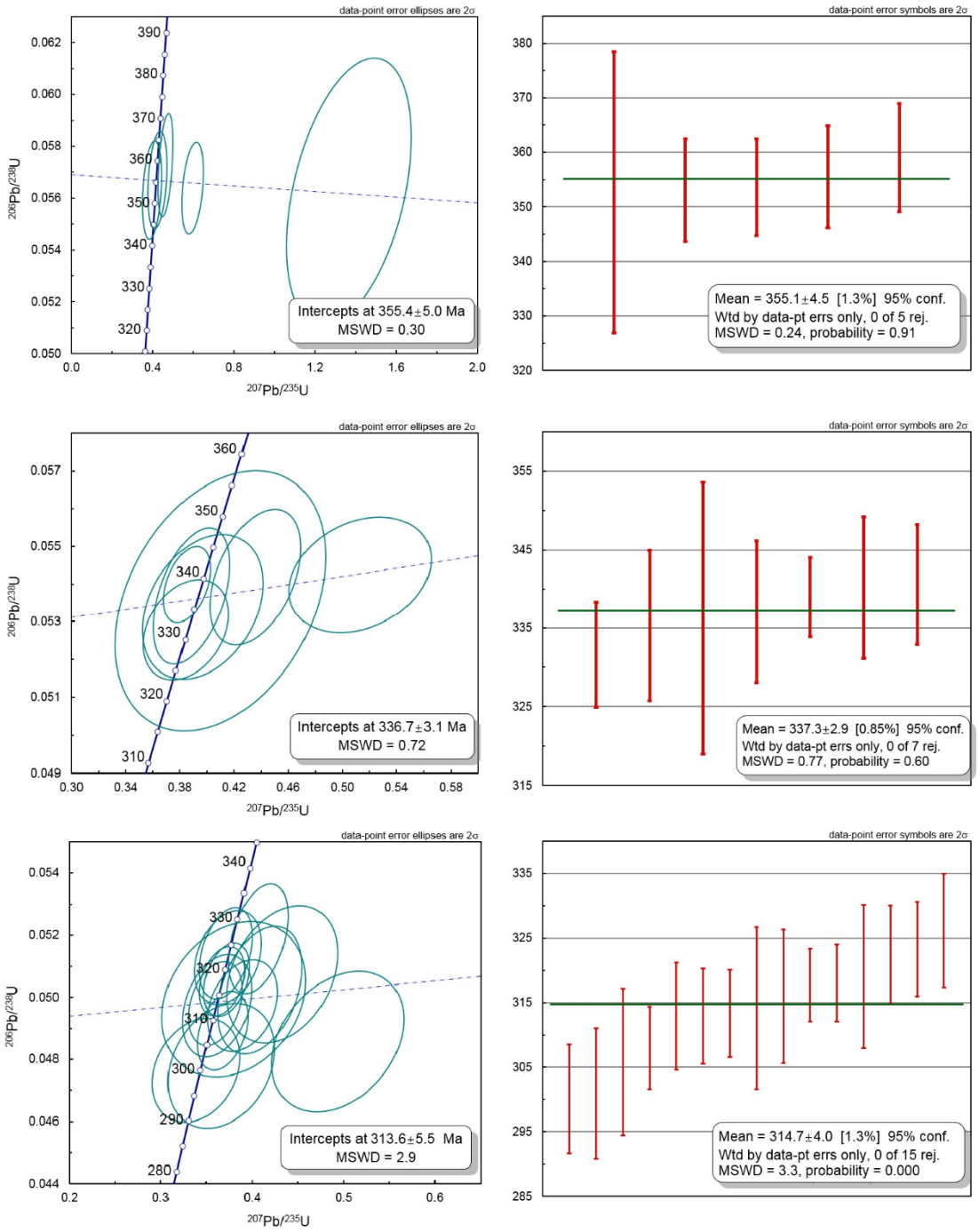

Figure 9. *Cont*.

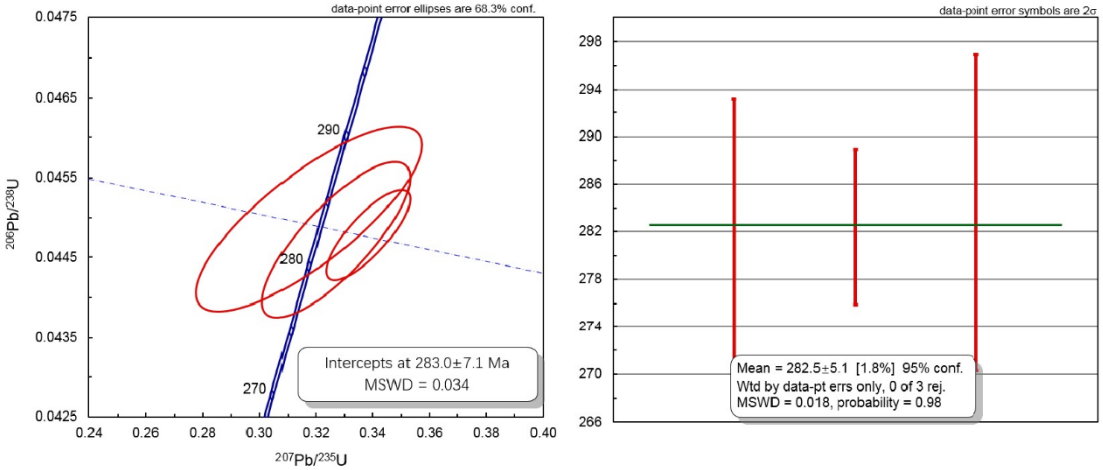

Figure 9. Concordia and weighted mean diagrams for U–Pb ages of zircon grains in vein H10-3. Error ellipses are shown at 1 σ. Weighted mean at 2 σ.

4.4. Zircon Trace Elements

A total of 20 trace element analyses were performed on 15 zircon grains from eclogite sample H11-5, including nine on inherited cores and the other 11 on metamorphic rims (Table S6). Li, P, Y, Nb, Ta, Th, and rare earth elements (REE) in rims were all obviously lower than that in cores. The cores of zircons showed positively sloping normalized chondrite REE patterns from the light rare earth elements (LREE) to the heavy rare earth elements (HREE), with positive Ce spikes and negative Eu anomalies (Figure 10), as is typical for magmatic zircons [69]. REE pattern of rims were relatively flat from the middle rare earth elements (MREE) to the HREE, resembling zircon crystallized in eclogitic facies metamorphosed rocks [69].

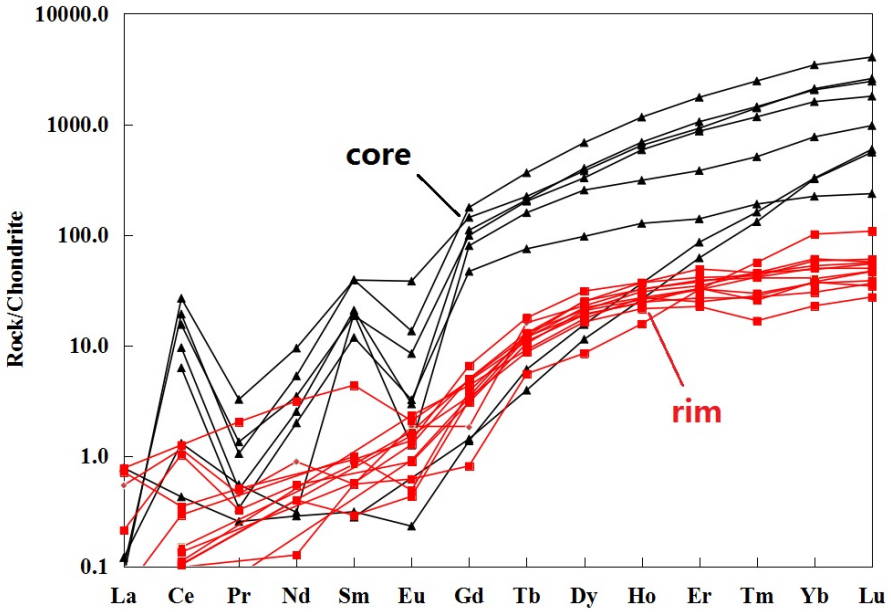

Figure 10. Chondrite-normalized rare earth element (REE) patterns for zircons in eclogite sample H11-5. Chondrite-normalization values were taken from [70].

Trace elements of zircon in vein sample H10-3 were obtained from the same spots of 30 U–Pb dating (Table S7). The zircon had 10 337–11 567 ppm Hf, 66.6–143.1 ppm Y, 0.08–0.67 ppm Nb, and 0.03–0.12 ppm Ta. The zircon grains had low LREE abundances, with some containing La and Pr at or below-detection-limit levels. In the chondrite-normalized diagram (Figure 11), four groups of zircons

all showed HREE enriched patterns. However, the Lu_N/Gd_N ratios showed a decrease from the first to the fourth group (from 25.97 to 18.42 in averages). The Eu_N/Eu_N^* ($Eu_N/(Sm_N*Gd_N)^{0.5}$) of four groups varied remarkably, ranging from 0.16 to 2.98.

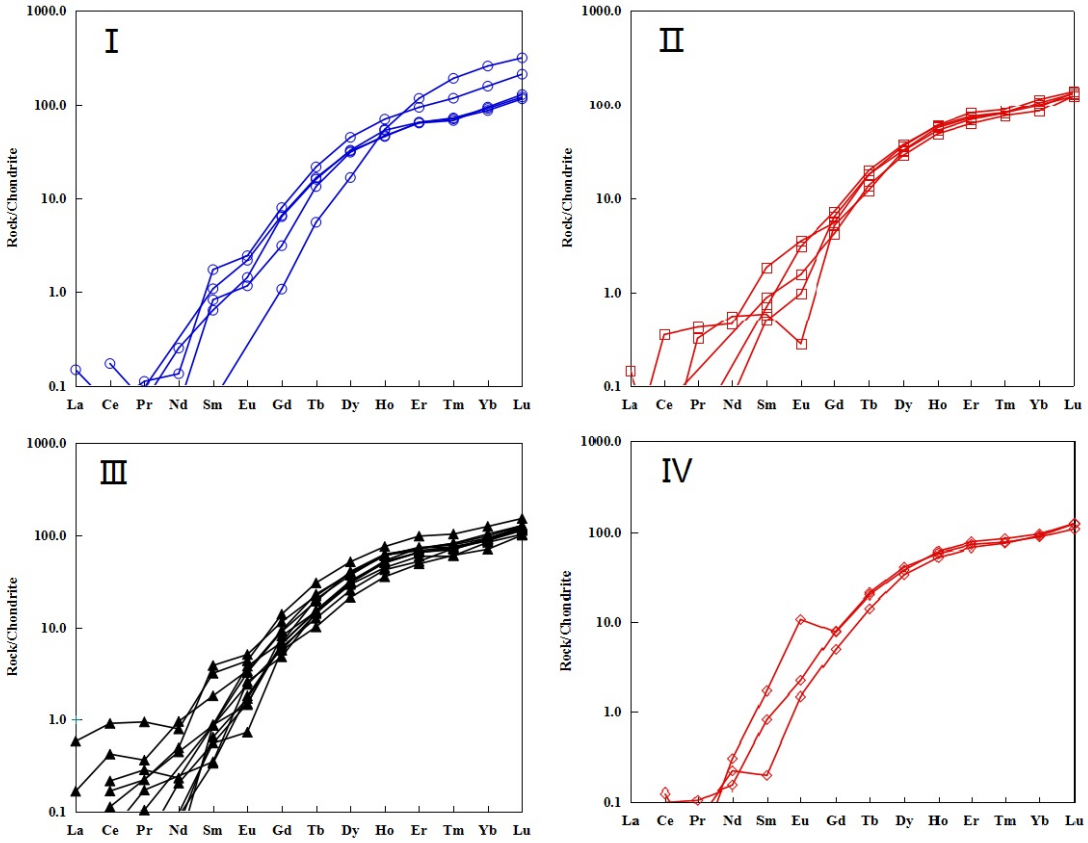

Figure 11. Chondrite-normalized REE patterns for zircons in vein sample H10-3. (**I**)–(**IV**) are denoted to Group I to Group IV zircon, respectively. Chondrite-normalization values were taken from [70].

5. Discussion

5.1. Metamorphic and Protolith Ages of Eclogite–Blueschist Belt in Southwestern Tianshan

Regarding the metamorphic ages of eclogite–bluschist belt in southwestern Tianshan, many Sm–Nd, Rb–Sr isochron ages, $^{40}Ar/^{39}Ar$ plateau ages, and U–Pb ages have been published (Table S8, [71–77]). The involved lithology included eclogite, blueschist, and mica schist, and most of the ages ranged in 310–350 Ma. Some researchers have considered that the eclogite facies metamorphic age should be about 345 Ma, and 330–310 Ma represent the stage of eclogite retrograded to blueschist and epidote–blueschist [58,74,78]. By SHRIMP zircon U–Pb dating, Zhang et al. [79] obtained 310–413 Ma for zircon core age and 226–233 Ma for zircon rim age in eclogites, and proposed that the Tarim block began to subduct in Permian and collided with Yili block in Triassic, which led to the debate on the subduction-collision time of southwestern Tianshan orogen.

More recently, many new data were reported for metamorphic ages of eclogite–bluschist belt in southwestern Tianshan, including Ph–(Ep)–whole rock Rb–Sr isochron ages of 313–309 Ma (blueschists having the peak assemblages Grt + Gln + Lws ± Omp; [56]), Lu–Hf isochron ages of 326–306 Ma (eclogites; [80]) and of 316–313 Ma (eclogites; [51]), SIMS zircon U–Pb ages of ~320 Ma (eclogites; [59,81]), SIMS rutile U–Pb age of 318 Ma (eclogites and vein; [58]), Sm–Nd isochron age of 319 Ma (eclogites; [55]) and of 305–310 Ma (eclogites; [82]), SHIRMP U–Pb zircon age of ~320 Ma (coesite bearing garnet–phengite schist; [45]), phengites $^{40}Ar/^{39}Ar$ plateau ages of 321.4 ± 1.6 and 318.6 ± 1.6 Ma (garnet glaucophane schist and garnet phengite schist; [83]), SIMS U–Pb perovskite age of 317 ± 11 Ma

or 308 ± 5 Ma (rodingitized mafic dikes included in UHP serpentinized ultramafic rocks; [84]). Tan et al. [85] linked the multistage zircon growth to garnet growth in a group of coesite-bearing eclogites for this UHP tectonic slice from UHP peak burial around 318.0 ± 2.3 Ma to HP peak metamorphism at 316.8 ± 0.8 Ma, then, with eclogite facies deformation at 312 ± 2.5 Ma. These ages dated eclogite facies minerals, e.g., omphacite, garnet, phengite, and rutile, or zircon rim with these mineral inclusions, and showed a narrow timespan of 320–305 Ma. Therefore, they were interpreted to reflect eclogite facies metamorphism. The eclogite facies metamorphic ages of eclogite–bluschist belt in southwestern Tianshan came to an agreement of 320–305 Ma, as recently summarized by [85–87].

In this study, the euhedral prismatic habit, core-rim structure and zoning feature of zircon in H11-5 eclogite were exactly the same as zircon in quartz vein from Sesia–Lanzo Zone of western Alps [21] and the Dabie orogen [30]. The zoning feature of the zircon rim was also similar to zircon crystallized in metamorphic veins from other orogens [14,26]. Although our zircons were extracted from eclogite, but not from the vein, the existence of a large number of veins in the eclogite–blueschist belt indicate that there were intensive fluid action during HP–UHP metamorphism [11,13,16,19,20,61,62,88–90]. Therefore, zircon rims in H11-5 eclogite were very likely to be grown from environment rich in fluid. The low content of Th (≤1.5 ppm) and Th/U ratios (0.001–0.019) are also consistent with zircon grown from metamorphic fluid [21]. Rutile, omphacite, and phengite as inclusions in zircon rim (Figure 5) indicate that the age of 311 ± 3 Ma dated eclogite facies metamorphism. This age further confirms that the eclogite facies metamorphic ages of the eclogite–bluschist belt in southwestern Tianshan must be in the range of 320–305 Ma.

The zircon cores of H11-5 eclogite have various internal structures with incomplete crystal morphology or corrode harbor morphology, indicating that the zircon cores should be crystallized from protolith magma or inherited from detrital residual. Zircon cores in this study yielded concordant $^{206}Pb/^{238}U$ apparent ages ranging from 413 ± 4 to 2326 ± 18 Ma, which can be divided into three groups: 2326 ± 18–2198 ± 28 Ma, 1220 ± 9–519 ± 5 Ma, and 451 ± 4–413 ± 4 Ma. Zircon cores in two eclogites in [59] gave two groups of age range: 2450 ± 31–1956 ± 26 Ma and 486 ± 8–428 ± 6 Ma. The inherited cores of zircons in eclogite in [45] yielded U–Pb apparent ages ranging from 802 Ma to 2919 Ma. In one eclogite sample in [81], the core domains of zircon grains with magmatic oscillatory zoning yielded a U–Pb concordia age of 454 ± 9 Ma, and the inherited cores of some zircon grains had apparent U–Pb ages between 609 Ma and 2305 Ma. Taken together, the large range (from ~410 Ma to ~2920 Ma) of U–Pb ages of zircon cores in eclogites indicate that the source rock of the eclogite–bluschist belt in southwestern Tianshan is very complex. Besides a Late Ordovician age for the eclogites' protolith, Precambrian continental crustal materials have also been involved in the formation of the eclogite samples' protoliths [81].

5.2. Timing of Episodic Fluid Action

Extensive studies have been conducted on various veins within HP–UHP metabasites in oceanic subduction zones [8,10,13,14]. These studies unraveled that different stages of veining may occur in the same HP to UHP metamorphic slices [15,17]. Hydrothermally crystallized zircon has been reported from different stages of vein related to HP–UHP metamorphism: (1) Prograde veins [13,21,26], (2) peak veins [14], and retrograde veins [12,27,30–33,91,92]. These zircons are often used to determine the formation age of veins in HP–UHP rocks, i.e., the time of fluid action during HP–UHP metamorphism. From these previous studies, it was found that zircon in veins from subducted oceanic crust often date prograde or peak metamorphism with fluid action [14,21,26], whereas zircon in veins from continental subducted orogen often date retrograde fluid action [12,27–31,92]. Furthermore, zircon in retrograde veins within continental collision orogen often yielded two age groups or protracted ages [12,28,30,31,92]. Thus, the two age groups from the vein are thought to date two episodes of fluid flow involving zircon growth during exhumation, or suggest protracted zircon growth during exhumation of the deeply subducted continental crust. In this study, zircon in vein sample H10-3

yielded four age groups, which might date four episodes of fluid flow involving zircon growth during subduction, peak metamorphism, and exhumation of the deeply subducted oceanic crust.

Zircon extracted from vein sample H10-3 had a euhedral, short-prismatic habit, weak luminescence internal with sector zoning, and a brighter rim with no zoning and without inherited core. These characteristics are clearly distinct from those of zircon recovered from eclogite H11-5 but resemble zircon crystallized from metamorphic fluid [14,24,26,27]. Thus, we can exclude the possibility that the vein zircon was brought from eclogite but precipitated from aqueous fluid. The Group IIIages (~315 Ma) were similar to zircon rim ages in eclogite H11-5 and also fell in the range of 320–305 Ma, which should be interpreted as eclogite facies metamorphic ages [86–88]. Group I (~355 Ma) and Group II (~337 Ma) ages were apparently higher than the recognized eclogite facies metamorphic ages. Some previous $^{40}Ar/^{39}Ar$ plateau and K–Ar ages of glaucophane and phengite from eclogites and blueschists from Chinese southwestern Tianshan also gave an older age range, from 415–331 Ma. However, these ages were attributed to incorporation of excess ^{40}Ar to varying degrees [58,59]. The authors of [42] reported Sm–Nd isochron ages of 343 ± 44 Ma (Grt–Gln–Omp–whole rock), 346 ± 3 Ma (Grt–Gln), and 333 ± 5 Ma (Grt–Omp) for an eclogite sample. The large error of the first one likely indicated isotopic disequilibrium between minerals and whole rock. Instead, the Grt–Gln pair and the Grt–Omp pair may represent prograde or near-peak eclogite facies metamorphism, and therefore 346 ± 3–333 ± 5 Ma may determine a period of prograde eclogite facies metamorphism [82]. In conjunction with published geochronology, [82] proposed that the subduction of the South Tianshan paleo-ocean began before 346 Ma, and that prograde blueschist to near eclogite facies metamorphism of the subducting oceanic crust occurred at 346–333 Ma. Our first two groups of ages (~355 Ma and ~337 Ma) are comparable to these Sm–Nd ages [40]. Thus, they can be interpreted to date two prograde events prior to eclogite facies metamorphism. The well-preserved prograde grossular and pyrope zoning of garnet in vein (Figure 3B, Table S1) also support this inference.

Group IV ages (~283 Ma) were apparently lower than the other three groups. This age is well-consistent with an age of 280.5 ± 4.3 Ma obtained from eclogite zircon rims by [85], which was thought to be dated the late exhumation movements after a greenschist facies metamorphism, since a greenschist facies Ar–Ar plateau age of 293.1 ± 1.7 Ma was reported by [83] for an epidote mica schist.

A collisional orogen is generally characterized by widespread development of subduction-related, syn-collisional, and post-collisional magmatism. The northward subduction of the South Tianshan paleo-ocean underneath Yili central Tianshan may start at Early Silurian and last until Early Carboniferous, producing a series of continental arc along the southern margin of Yili-central Tianshan block [93–95]. There are a lot of mafic to felsic magmatic plutons and volcanic rocks related to continental arc from Early Silurian to Late Carboniferous (ranging from ~450 Ma to ~320 Ma) reported in the South Tianshan orogen ([96–98] and references therein). There are also lots of syn-collisional and post-collisional magmatism (ranging from ~320 Ma to ~270 Ma) reported along this orogen ([99,100] and references therein). Detrital zircons collected from rivers originating from the Chinese South Tianshan yielded four distinct age populations of 500–460 Ma, 450–390 Ma, 360–320 Ma, and 300–270 Ma, indicating the major magmatic events in this orogen. The 450–390 Ma and 360–320 events were closely related to the northward subduction of the South Tianshan Ocean, while the 300–270 magmatic event is thought to post-date the closure of the South Tianshan Ocean [13,101,102].

Based on the occurrence of HP–UHP belt together with discovery of coeval low-P granulite facies rocks to the north, a paired metamorphic belt tectonic model was proposed for the south Tianshan [35,50,79,94]. Detailed studies of petrological and U–Pb zircon dating have been conducted on the migmatites and granulites in its high dT/dP (geothermic gradient) part. For the migmatites, recrystallized zircon has been transformed from pre-existing zircon under subsolidus conditions at ~400 Ma and ~360 Ma. Metamorphic rims have grown on zircons at ~400 Ma, ~290Ma and ~270 Ma, corresponding to three phases of anatexis [94]. For the HP felsic and mafic granulites, three stages of metamorphism have been revealed: Stage I granulite facies metamorphism (~390 Ma) may be related to the Devonian arc magmatic intrusion, Stage II HP granulite facies metamorphism

(350–340 Ma) may due to the involvement of being captured into the subducting slab and experienced the high-pressure metamorphism, and Stage IIIamphibolite facies metamorphism occurred at ~320 Ma during exhumation [96,97].

The four groups of age (~355 Ma, ~337 Ma, 315 Ma, and ~ 283Ma) gained in vein sample H10-3 are comparable to the above subduction-related, syn-collisional, and post-collisional magmatic events reported along the South Tianshan Orogen, and are also comparable to the metamorphic events reported in the paired metamorphic belt, so it is reasonable to interpret these ages as prograde metamorphism related to the cold subduction of the South Tianshan paleo-ocean, eclogite facies metamorphism related to the collision between the Tarim plate and the Paleo-Kazakhstan continent, and post-greenschist facies metamorphism related to the exhumation near the surface. Here, we proposed that subduction of the South Tianshan paleo-ocean may have begun at ~360Ma, prograde blueschist facies metamorphism of the subducting oceanic crust occurred at ~340 Ma, peak eclogite facies metamorphism at 320–305 Ma, greenschist facies retrograde metamorphism at ~290 Ma, and succedent a later retrograde metamorphism at ~280 Ma. All these prograde, peak, and retrograde metamorphisms may have been accompanied with fluid actions.

5.3. Source and Characteristics of the Fluid

Different stages of veining occur in the same HP to UHP metamorphic slices, suggesting that the origin of vein-forming fluids is complicated, and both internal and external fluids may be involved in veining [15,17]. These observations and interpretations have significantly improved our understanding of fluid behavior during subduction of the oceanic crust. Studies have shown that except for the ability of each element enter the crystal lattice, trace elements characteristic of metamorphic overgrowth or newly growth zircon is also controlled by the minerals formed simultaneously with zircon (e.g., garnet, plagioclase, epidote and rutile) [14,21,103]. For example, in epidote–amphibolite facies, HREE-rich garnet cannot stabilize, but LREE-rich epidote and Eu-rich plagioclase are coexisting minerals, so the metamorphic zircon grow in amphibolite facies has the characteristic of relatively rich in HREE and obvious negative Eu anomalies. However, in eclogite facies, HREE-rich garnet is stabilized, but the plagioclase is absence, so the metamorphic zircon grows in eclogite facies has the characteristic of relatively deplete in HREE with no obvious negative Eu anomalies. If the metamorphic zircon is grown simultaneously with rutile or later than rutile, which is rich in Nb and Ta with high Nb/Ta ratio, these zircons will have low Nb and Ta content and a low Nb/Ta ratio [14,103–105]. In addition, the trace element characteristic of metamorphic zircon is also related to whether the growth system is closed or not. If the metamorphic zircon is grown in open system, the influence of paragenetic minerals weakened, e.g., zircon growth with garnet may not show depletion in HREE [103,105].

Although zircon in vein H10-3 yields four age groups, they have similar morphology and internal structure, indicating that they were grown in similar fluid conditions. These zircons also have similar trace elements and rare earth elemental patterns, and only the Lu_N/Gd_N ratio reduced with age, i.e., the enrichment degree of HREE reduced with age. According to the studies mentioned above, zircon with the first age group (~355 Ma) may grow in the prograde epidote–amphibolite facies, and zircon with the second age group (~337 Ma) may grow in the prograde amphibolite or blueschist facies. Zircon grown in these two stages are rich in HREE because the garnet is not yet formed at that time. Zircon with the third age group date and eclogite facies metamorphic age are still rich in HREE. We speculate that these zircons may grow in an open system. The prograde veining fluid in HP–UHP terrene of southeastern Tianshan comes both from surrounding eclogite itself (e.g., [11]) and from external fluid [16], so it could not be a closed system. The variation of Eu_N/Eu_N^* (range from 0.16 to 2.98 for the four groups of vein zircons) also support this speculation. Our speculation is also supported by the chondrite-normalized REE patterns of every age group of zircons from sample H10-3, which are not exactly similar (or parallel) to each other. This suggests that various process or fluids were involved in the formation of each group of zircons. Although the metamorphic zircon may co-crystallize with HREE-enriched garnet due to the infiltration of external fluid, the formation of garnet would not

cause the significant locally depletion of HREE, and the co-crystallized metamorphic zircon would not deplete in HREE. In general, with the evolution of metamorphism, the content of garnet increased, and the content has a significant influence on HREE, thus leading to the reduce of Lu_N/Gd_N of zircon from Group I to the Group III. In addition, the low content of Nb and Ta and low Nb/Ta ratio of these three groups of zircons indicate that rutile was formed during the formation of metamorphic zircon [14,103–105]. From the statistics of stochastic analysis of these zircon, the third group of zircon has the largest number. This may indicate that the intensity of the third episode of fluid action was the largest, or the concentration of Zr in this episode of fluid action was the maximum, thus resulted in a large numbers of zircon formation in vein and in eclogite with the age of 320–310 Ma.

Zircon, rutile, garnet, and epidote as mineral assemblage coexisting in vein and the characteristic of HREE enrich in zircon suggest that the vein-forming fluid should be enriched in the high field strength element (HFSE) and HREE, indicating that HFSE and HREE, which are traditionally considered as immobile elements [6,106,107], have relatively high solubility and activity in appropriate conditions. Based on the observation of rutile-bearing vein and segregation within eclogite [11] and P–T estimates of 570 °C to 630 °C and 2.7 GPa to 3.3 GPa for peak eclogite facies metamorphism [42], Xia et al. [108] argued for involvement of supercritical fluid for the HFSE transport and the subsequent precipitation of rutile in HP veins at such LT/UHP conditions. However, the ages and trace element characteristics of vein zircon in this study show that fluid action was enriched in HFSE and HREE during the epidote–amphibolite facies metamorphism with lower P–T conditions. In addition, rutile and garnet also coexist in many retrograde veins in eclogite–blueschist belt from southwestern Tianshan [19,20]. Thus, the P–T conditions for dissolving and transporting HFSE and HREE could be lower than previously thought and do not necessarily involve a supercritical fluid. The apatite in the vein had high F content (average in 2.67 wt.%, Table S2), and Nb, Ta had high solubility in F rich hydrothermal fluid [109]. Thus, we suggest that the high F content in the fluid should have played a significant role in the forming of rutile-bearing veins.

6. Conclusions

The morphology and internal structure of zircon in eclogite and vein indicate that these zircons were crystallized from metamorphic fluid. Both zircon in eclogite and vein recorded eclogite facies were metamorphism age (320–310 Ma). The inherited core of zircon in eclogite gave a large range of ages (412–2919 Ma), suggested that source rock of the eclogite–bluschist belt in southwestern Tianshan was very complex.

The vein zircon yielded four groups of age (~355 Ma, ~337 Ma, ~315 Ma, and ~283 Ma), which dated four episodes of fluid flow involving zircon growth. The first two groups of age may represent the prograde epidote–amphibolite facies and amphibolite/blueschist facies metamorphism stage, respectively. The third group dates the eclogitic facie metamorphism, and the fourth dates a retrograde metamorphism after greenschist facies. Trace elements of vein zircon and mineral assemblage of vein suggest that the vein-forming fluid system should be an open system. The coexistance of rutile, zircon, and garnet in the prograde vein and the HREE enrichment characteristic of vein zircon suggested that the vein-forming fluids were enriched in HFSE and HREE and such fluid could be formed under low P–T condition.

There are plenty of prograde and retrograde vein in the eclogite–bluschist belt in southwestern Tianshan. Our preliminary study suggest that vein zircon can provide not only the age of various metamorphism stages, but also the time of episodes fluid action during oceanic subduction-exhumation, as well the provenance of these fluid actions.

Supplementary Materials: The following are available online at http://www.mdpi.com/2075-163X/9/12/727/s1, Table S1: Representative EMP analyses of minerals in vein H10-3, Table S2: Representative EMP analyses of apatite in vein H10-3, Table S3: Representative EMP analyses of mineral inclusion in zircons in eclogite H11-5 and vein H10-3, Table S4: Zircon U–Pb isotopic data obtained by LA-ICP-MS for eclogite H11-5, Table S5: Zircon U–Pb isotopic data obtained by LA-ICP-MS for vein H10-3, Table S6: LA-ICP-MS trace element analyses for zircon in

eclogite H11-5, Table S7: LA-ICP-MS trace element analyses for zircon in vein H10-3, Table S8. Geochronology data of eclogite–blueschist belt in southwestern Tianshan.

Author Contributions: Sample collection and article writing, Z.-Y.C.; English writing, Z.-Y.C.; Figures drawing, Z.-Y.C. and Z.L.; Discussion, Z.-Y.C., L.-F.Z., Z.L. and J.-X.D.; Research method, Z.-Y.C., and L.-F.Z.; Experimental design, Z.-Y.C. and L.-F.Z.; Experimental data analysis, Z.-Y.C.

Funding: This study was supported by National Natural Science Foundation of China (NSFC Grants 41372074 and 41330210).

Acknowledgments: Hu Zhaochu, Zong Keqing and Hou Kejun are gratefully acknowledged for assistance with zircon analyses with LA-ICP-MS. The authors would like to thank the editors and the anonymous reviewers for their helpful and constructive comments.

Conflicts of Interest: The authors declare no conflict of interest.

References

1. Agard, P.; Goffé, B.; Touret, J.L.R.; Vidal, O. Retrograde mineral and fluid evolution in high-pressure metapelites (Schistes lustrés unit, Western Alps). *Contrib. Mineral. Petrol.* **2000**, *140*, 296–315. [CrossRef]
2. Miller, C.; Zanetti, A.; Thöni, M. Eclogitisation of gabbroic rocks: Redistribution of trace elements and Zr in rutile thermometry in an Eo-Alpine subduction zone (Eastern Alps). *Chem. Geol.* **2002**, *239*, 96–123. [CrossRef]
3. John, T.; Schenk, V. Partial eclogitisation of gabbroic rocks in a late Precambrian subduction zone (Zambia): Prograde metamorphism triggered by fluid infiltration. *Contrib. Mineral. Petrol.* **2003**, *146*, 174–191. [CrossRef]
4. Hermann, J.; Spandler, C.; Hack, A.; Korsakov, A.V. Aqueous fluids and hydrous melts in high-pressure and ultrahigh pressure rocks: Implications for element transfer in subduction zones. *Lithos* **2006**, *92*, 399–417. [CrossRef]
5. Scambelluri, M.; Philippot, P. Deep fluids in subduction zones. *Lithos* **2001**, *55*, 213–227. [CrossRef]
6. Zheng, Y.F. Fluid regime in continental subduction zones: Petrological insights from ultrahigh-pressure metamorphic rocks. *J. Geol. Soc.* **2009**, *166*, 763–782. [CrossRef]
7. Zheng, Y.F.; Gao, X.Y.; Chen, R.X.; Gao, T.S. Zr-in-rutile thermometry of eclogite in the Dabie orogen: Constraints on rutile growth during continental subduction-zone metamorphism. *J. Asian Earth Sci.* **2011**, *40*, 427–451. [CrossRef]
8. Becker, H.; Jochum, K.P.; Carlson, R.W. Constraints from high-pressure veins in eclogites on the composition of hydrous fluids in subduction zones. *Chem. Geol.* **1999**, *160*, 291–308. [CrossRef]
9. Franz, L.; Romer, R.L.; Klemd, R.; Schmid, R.; Oberhaensli, R.; Wagner, T.; Shuwen, D. Eclogite-facies quartz veins within metabasites of the Dabie Shan (eastern China): Pressure–temperature–time–deformation path, composition of the fluid phase and fluid flow during exhumation of high-pressure rocks. *Contrib. Mineral. Petrol.* **2001**, *141*, 322–346. [CrossRef]
10. Widmer, T.; Thompson, A.B. Local origin of high pressure vein material in eclogite facies rocks of the Zermatt-Saas Zone 2001, Switzerland. *Am. J. Sci.* **2001**, *301*, 627–656. [CrossRef]
11. Gao, J.; John, T.; Klemd, R.; Xiong, X.M. Mobilization of Ti–Nb–Ta during subdution: Evidence from rutile-bearing dehydration segregations and veins hosted in eclogite, Tianshan, NW China. *Geochim. Cosmochim. Acta* **2007**, *71*, 4974–4996. [CrossRef]
12. Zheng, Y.F.; Gao, T.S.; Wu, Y.B. Fluid flow during exhumation of deeply subducted continental crust: Zircon U–Pb age and O isotope studies of a quartz vein within ultrahigh-pressure eclogite. *J. Metamorph. Geol.* **2007**, *25*, 267–283. [CrossRef]
13. Philippot, P.; Selverstone, J. Trace-element-rich brines in eclogitic veins: Implications for fluid composition and transport during subduction. *Contrib. Mineral. Petrol.* **1991**, *106*, 417–430. [CrossRef]
14. Rubatto, D.; Hermann, J. Zircon formation during fluid circulation in eclogites (Monviso, Western Alps): Implications for Zr and Hf budget in subduction zones. *Geochim. Cosmochim. Acta* **2003**, *67*, 2173–2187. [CrossRef]
15. Spandler, C.; Hermann, J. High-pressure veins in eclogite from New Caledonia and their significance for fluid migration and seismic activity in subduction zones. *Lithos* **2006**, *89*, 135–153. [CrossRef]

16. John, T.; Klemd, R.; Gao, J.; Garbe-Schönberg, C.D. Trace-element mobilization in slabs due to non steady-state fluid–rock interaction: Constraints from an eclogite-facies transport vein in blueschist (Tianshan, China). *Lithos* **2008**, *103*, 1–24. [CrossRef]
17. Spandler, C.; Pettke, T.; Rubatto, D. Internal and external fluid sources for eclogite-facies veins in the Monviso Meta-ophiolite, Western Alps: Implications for fluid flow in subduction zones. *J. Petrol.* **2011**, *52*, 1207–1236. [CrossRef]
18. Van der Straaten, F.; Schenk, V.; John, T.; Gao, J. Blueschist-facies rehydration of eclogites (Tian Shan, NW-China): Implications for fluid–rock interaction in the subduction channel. *Chem. Geol.* **2008**, *255*, 195–219. [CrossRef]
19. Lü, Z.; Zhang, L.F.; Du, J.X.; Yang, X.; Tian, Z.L.; Xia, B. Petrology of HP metamorphic veins in coesite-bearing eclogite from western Tianshan, China: Fluid processes and elemental mobility during exhumation in a cold subduction zone. *Lithos* **2012**, *136*, 168–186. [CrossRef]
20. Chen, Z.Y.; Zhang, L.F.; Du, J.X.; Lü, Z. Zr-in-rutile thermometry in eclogite and vein from southwestern Tianshan, China. *J. Asian Earth Sci.* **2013**, *63*, 70–80. [CrossRef]
21. Rubatto, D.; Gebauer, D.; Compagnoni, R. Dating of eclogite-facies zircons: The age of Alpine metamorphism in the Sesia–Lanzo Zone (Western Alps). *Earth Planet. Sci. Lett.* **1999**, *167*, 141–158. [CrossRef]
22. Ayers, J.C.; Dunkle, S.; Gao, S.; Miller, C.E. Constraints on timing of peak and retrograde metamorphism in the Dabie Shan ultrahigh-pressure metamorphic belt, east–central China, using U–Th–Pb dating of zircon and monazite. *Chem. Geol.* **2002**, *186*, 315–331. [CrossRef]
23. Corfu, F.; Hanchar, J.M.; Hoskin, P.W.O.; Kinny, P. Altas of zircon textures. In *Zircon: Reviews in Mineralogy and Geochemistry*; Hanchar, J.M., Hoskin, P.W.O., Eds.; Mineralogical Society of America: Chantilly, VA, USA, 2003; Volume 53, pp. 469–500.
24. Zheng, Y.F.; Wu, Y.B.; Chen, F.K.; Gong, B.; Li, L.; Zhao, Z.F. Zircon U–Pb and oxygen isotope evidence for a large-scale ^{18}O depletion event in igneous rocks during the Neoproterozoic. *Geochim. Cosmochim. Acta* **2004**, *68*, 4145–4165. [CrossRef]
25. Liu, F.L.; Liou, J.G. Zircon as the best mineral for P–T–time history of UHP metamorphism: A review on mineral inclusions and U–Pb SHRIMP ages of zircons from the Dabie–Sulu UHP rocks. *J. Asian Earth Sci.* **2011**, *40*, 1–39. [CrossRef]
26. Liati, A.; Gebauer, D. Constraining the prograde and retrograde P–T–t path of Eocene HP rocks by SHRIMP dating of different zircon domains: Inferred rates of heating, burial, cooling and exhumation for central Rhodope, northern Greece. *Contrib. Mineral. Petrol.* **1999**, *135*, 340–354. [CrossRef]
27. Wu, Y.B.; Gao, S.; Zhang, H.F.; Yang, S.H.; Liu, X.C.; Jiao, W.F.; Liu, Y.S.; Yuan, H.L.; Gong, H.J.; He, M.C. U–Pb age, trace-element, and Hf-isotope compositions of zircon in a quartz vein from eclogite in the western Dabie Mountains: Constraints on fluid flow during early exhumation of ultrahigh-pressure rocks. *Am. Mineral.* **2009**, *94*, 303–312. [CrossRef]
28. Chen, R.X.; Zheng, Y.F.; Hu, Z.C. Episodic fluid action during exhumation of deeply subducted continental crust: Geochemical constraints from zoisite–quartz vein and host metabasite in the Dabie orogen. *Lithos* **2012**, *155*, 146–166. [CrossRef]
29. Chen, R.X.; Zheng, Y.F. Zirconological records of fluid/melt action during continental subduction-zone metamorphism. *Chin. Sci. Bull.* **2013**, *58*, 2227–2232. [CrossRef]
30. Sheng, Y.M.; Zheng, Y.F.; Chen, R.X.; Li, Q.L.; Dai, M.N. Fluid action on zircon growth and recrystallization during quartz veining within UHP eclogite: Insights from U–Pb ages, O–Hf isotopes and trace elements. *Lithos* **2012**, *136*, 126–144. [CrossRef]
31. Sheng, Y.M.; Zheng, Y.F.; Li, S.N.; Hu, Z.C. Element mobility during continental collision: Insights from polymineralic metamorphic vein within UHP eclogite in the Dabie orogeny. *J. Metamorph. Geol.* **2013**, *31*, 221–241. [CrossRef]
32. Beinlich, A.; Klemd, R.; John, T.; Gao, J. Trace-element mobilization during Ca-metasomatism along a major fluid conduit: Eclogitization of blueschist as a consequence of fluid–rock interaction. *Geochim. Cosmochim. Acta* **2010**, *74*, 1892–1922. [CrossRef]
33. Gao, J.; Li, M.; He, G.; Xiao, X. Paleozoic tectonic evolution of the Tianshan Orogen, northwestern China. *Tectonophysics* **1998**, *287*, 213–231. [CrossRef]
34. Windley, B.F.; Allen, M.B.; Zhang, C.; Zhao, Z.; Wang, G. Paleozoic accretion and Cenozoic redeformation of the Chinese Tien Shan range, central Asia. *Geology* **1990**, *18*, 128–131. [CrossRef]

35. Li, Q.; Zhang, L.F. The PT path and geological signifificance of low-pressure granulite-facies metamorphism in Muzhaerte, southwestern Tianshan, Xinjiang, China. *Acta Petrol. Sin.* **2004**, *20*, 583–594.
36. Zhang, L.F.; Lü, Z.; Zhang, G.B.; Song, S.G. The geological characteristics of oceanic type UHP metamorphic belts and their tectonic implications: Case studies from Southwest Tianshan and North Qaidam in NW China. *Chin. Sci. Bull.* **2008**, *53*, 3120–3130. [CrossRef]
37. Gao, J.; Klemd, R.; Zhang, L.; Wang, Z.; Xiao, X. P–T path of high-pressure/low-temperature rocks and tectonic implications in the western Tianshan Mountains, NW China. *J. Metamorph. Geol.* **1999**, *17*, 621–636. [CrossRef]
38. Klemd, R.; Schroter, F.C.; Will, T.M.; Gao, J. P–T evolution of glaucophane–omphacite bearing HP–LT rocks in the western Tianshan Orogen, NW China: New evidence for 'Alpine-type' tectonics. *J. Metamorph. Geol.* **2002**, *20*, 239–254. [CrossRef]
39. Zhang, L.F.; Ai, Y.L.; Song, S.G.; Liou, J.; Wei, C.J. A brief review of UHP metaophiolitic rocks, southwestern Tianshan, western China. *Int. Geol. Rev.* **2007**, *49*, 811–823. [CrossRef]
40. Gao, J.; Klemd, R. Formation of HP–LT rocks and their tectonic implications in the southwestern Tianshan Orogen, NW China: Geochemical and age constraints. *Lithos* **2003**, *66*, 1–22. [CrossRef]
41. Ai, Y.L.; Zhang, L.F.; Li, X.P.; Qu, J.F. Geochemical characteristics and tectonic implications of HP–UHP eclogites and blueschists in southwestern Tianshan, China. *Prog. Nat. Sci.* **2006**, *16*, 624–632. (In Chinese with English Abstract)
42. Lü, Z.; Zhang, L.F.; Du, J.X.; Bucher, K. Coesite inclusions in garnet from eclogitic rocks in southwestern Tianshan, northwest China: Convincing proof of UHP metamorphism. *Am. Mineral.* **2008**, *93*, 1845–1850. [CrossRef]
43. Lü, Z.; Zhang, L.F.; Du, J.X.; Bucher, K. Petrology of coesite-bearing eclogite from Habutengsu Valley, southwestern Tianshan, NW China and its tectonometamorphic implication. *J. Metamorph. Geol.* **2009**, *27*, 773–787. [CrossRef]
44. Lü, Z.; Zhang, L.F. Coesite in the eclogite and schist of the Atantayi Valley 2009, southwestern Tianshan, China. *Chin. Sci. Bull.* **2012**, *57*, 1467–1472. [CrossRef]
45. Yang, X.; Zhang, L.F.; Tian, Z.L.; Bader, T. Petrology and U–Pb zircon dating of coesitebearing metapelites from the Kebuerte Valley, southwestern Tianshan, China. *J. Asian Earth Sci.* **2013**, *70*, 295–307. [CrossRef]
46. Tian, Z.L.; Wei, C.J.; Zhang, Z.M. Petrology and metamorphic P–T path of coesite-bearing politic schist from southwestern Tianshan Mountains, Xinjiang. *Acta Petrol. Mineral.* **2016**, *35*, 265–275. (In Chinese with English Abstract)
47. Zhang, L.F.; Ellis, D.J.; Jiang, W.B. Ultrahigh-pressure metamorphism in southwestern Tianshan, China: Part I. Evidence from inclusions of coesite pseudomorphs in garnet and from quartz exsolution lamellae in omphacite in eclogites. *Am. Mineral.* **2002**, *87*, 853–860. [CrossRef]
48. Zhang, L.F.; Ellis, D.J.; Williams, S. Ultra-high pressure metamorphism in southwestern Tianshan, China: Part II. Evidence from magnesite in eclogite. *Am. Mineral.* **2002**, *87*, 861–866. [CrossRef]
49. Zhang, L.F.; Ellis, D.J.; Arculus, R.J. 'Forbidden zone' subduction of sediments to 150 km depth—The reaction of dolomite to magnesite plus aragonite in the UHPM metapelites from southwestern Tianshan, China. *J. Metamorph. Geol.* **2003**, *21*, 523–529. [CrossRef]
50. Zhang, L.F.; Du, J.X.; Lü, Z. A huge oceanic-type UHP metamorphic belt in southwestern Tianshan, China: Peak metamorphic age and P–T path. *Chin. Sci. Bull.* **2013**, *58*, 4378–4383. [CrossRef]
51. Klemd, R.; John, T.; Scherer, E.E.; Rondenay, S.; Gao, J. Changes in dip of subducted slabs at depth: Petrological and geochronological evidence from HP–UHP rocks (Tianshan, NW-China). *Earth Planet. Sci. Lett.* **2011**, *310*, 9–20. [CrossRef]
52. Wei, C.; Powell, R.; Zhang, L.F. Eclogites from the south Tianshan, NW China: Petrological characteristic and calculated mineral equilibria in the Na_2O–CaO–FeO–MgO–Al_2O_3–SiO_2–H_2O system. *J. Metamorph. Geol.* **2003**, *21*, 163–179. [CrossRef]
53. Wei, C.J.; Wang, W.; Clarke, G.; Zhang, L.F.; Song, S.G. Metamorphism of high/ultrahigh-pressure pelitic–felsic schist in the South Tianshan Orogen, NW China: Phase equilibria and P–T path. *J. Petrol.* **2009**, *50*, 1973–1991. [CrossRef]
54. Gao, J.; He, G.; Li, M.; Xiao, X.; Tang, Y.; Wang, J.; Zhao, M. The mineralogy, petrology, metamorphic PTDt trajectory and exhumation mechanism of blueschists, south Tianshan, northwestern China. *Tectonophysics* **1995**, *250*, 15l–168. [CrossRef]

55. Hegner, E.; Klemd, R.; Kroner, A.; Corsini, M.; Alexeiev, D.V.; Iaccheri, L.M.; Zack, T.; Dulski, P.; Xia, X.; Windley, B.F. Mineral ages and PT conditions of Late Paleozoic high pressure eclogite and provenance of melange sediments from Atbashi in the south Tianshan orogen of Kyrgyzstan. *Am. J. Sci.* **2010**, *310*, 916–950. [CrossRef]
56. Klemd, R.; Brocker, M.; Hacker, B.R.; Gao, J.; Gans, P.; Wemmer, K. New age constraints on the metamorphic evolution of the high-pressure/low-temperature belt in the southwestern Tianshan Mountains, NW China. *J. Geol.* **2005**, *113*, 157–168. [CrossRef]
57. Simonov, V.A.; Sakiev, K.S.; Volkova, N.I.; Stupakov, S.I.; Travin, A.V. Conditions of formation of the Atbashi Ridge eclogites (South Tien Shan). *Russ. Geol. Geophys.* **2008**, *49*, 803–815. [CrossRef]
58. Li, Q.L.; Lin, W.; Su, W.; Li, X.H.; Shi, Y.H.; Liu, Y.; Tang, G.Q. SIMS U–Pb rutile age of low-temperature eclogites from southwestern Chinese Tianshan, NW China. *Lithos* **2010**, *122*, 76–86. [CrossRef]
59. Su, W.; Gao, J.; Klemd, R.; Li, J.L.; Zhang, X.; Li, X.H.; Chen, N.S.; Zhang, L. U–Pb zircon geochronology of Tianshan eclogites in NW China: Implication for the collision between the Yili and Tarim blocks of the southwestern Altaids. *Eur. J. Mineral.* **2010**, *22*, 473–478. [CrossRef]
60. van der Straaten, F.; Halama, R.; John, T.; Schenk, V.; Hauff, F.; Andersen, N. Tracing the effects of high-pressure metasomatic fluids and seawater alteration in blueschist facies overprinted eclogites: Implications for subduction channel processes. *Chem. Geol.* **2012**, *292*, 69–87. [CrossRef]
61. Gao, J.; Klemd, R. Primary fluids entrapped at blueschist to eclogite transition: Evidence from the Tianshan meta-subduction complex in northwestern China. *Contrib. Mineral. Petrol.* **2001**, *142*, 1–14. [CrossRef]
62. Zhang, L.J.; Zhang, L.F.; Lü, Z.; Bader, B.; Chen, Z. Nb–Ta mobility and fractionation during exhumation of UHP eclogites from southwestern Tianshan, China. *J. Asian Earth Sci.* **2016**, *122*, 136–157. [CrossRef]
63. Lü, Z.; Bucher, K.; Zhang, L.F.; Du, J.X. The Habutengsu metapelites and metagreywackes in southwestern Tianshan, China: Metamorphic evolution and tectonic implications. *J. Metamorph. Geol.* **2012**, *30*, 907–926. [CrossRef]
64. Liu, Y.S.; Hu, Z.C.; Gao, S.; Günther, D.; Xu, J.; Gao, C.G.; Chen, H.H. In situ analysis of major and trace elements of anhydrous minerals by LA–ICP–MS without applying an internal standard. *Chem. Geol.* **2008**, *257*, 34–43. [CrossRef]
65. Liu, Y.S.; Gao, S.; Hu, Z.C.; Gao, C.G.; Zong, K.Q.; Wang, D.B. Continental and oceanic crust recycling-induced melt-peridotite interactions in the Trans-North China Orogen: U–Pb dating, Hf isotopes and trace elements in zircons from mantle xenoliths. *J. Petrol.* **2010**, *51*, 537–571. [CrossRef]
66. Liu, Y.S.; Hu, Z.C.; Zong, K.Q.; Gao, C.G.; Gao, S.; Xu, J.; Chen, H.H. Reappraisement and refinement of zircon U–Pb isotope and trace element analyses by LA–ICP–MS. *Chin. Sci. Bull.* **2010**, *55*, 1535–1546. [CrossRef]
67. Wu, Y.B.; Zheng, Y.F. Genesis of zircon and its constraints on interpretation of U–Pb age. *Chin. Sci. Bull.* **2004**, *49*, 1554–1569. [CrossRef]
68. Williams, I.S.; Buick, I.S.; Cartwright, I. An extended episode of early Mesoproterozoic metamorphic fluid flow in the Reynolds Range, central Australia. *J. Metamorph. Geol.* **1996**, *14*, 29–47. [CrossRef]
69. Rubatto, D.; Liati, A.; Gebauer, D. Dating UHP metamorphism. *EMU Notes Mineral.* **2003**, *5*, 341–363.
70. Sun, S.S.; McDonough, W.F. Chemical and isotopic systematics of oceanic basalt: Implications for mantle composition and processes. In *Magmatism in the Ocean Basins*; Sanders, A.D., Norry, M.J., Eds.; Geological Society: London, UK, 1989; Volume 42, pp. 313–345.
71. Xiao, X.C.; Tang, Y.Q.; Li, J.Y. *Tectonic Structure of North Xinjiang and Adjacent Area*; Geology Press: Beijing, China, 1992; pp. 1–169. (In Chinese with English Abstract)
72. Tang, Y.Q.; Gao, J.; Zhao, M. *The Ophiolite and Blueschists in the Southwestern Tianshan Orogenic Belt Xinjiang Northwestern China*; Geological Publishing House: Beijing, China, 1995; pp. 1–133. (In Chinese)
73. Gao, J.; Zhang, L.; Liu, W. The Ar^{40}/Ar^{39} age record of formation and uplift of the blueschists and eclogites in the southwestern Tianshan mountains. *Chin. Sci. Bull.* **2000**, *45*, 1047–1052. [CrossRef]
74. Gao, J.; Long, L.L.; Qian, Q.; Huang, D.Z.; Su, W.; Klemd, R. South Tianshan: A Late Paleozoic or a Triassic orogen? *Acta Petrol. Sin.* **2006**, *22*, 1049–1061. (In Chinese with English Abstract)
75. John, T.; Gussone, N.; Podladchikov, Y.Y.; Bebout, G.E.; Dohmen, R.; Halama, R.; Klemd, R.; Magna, T.; Seitz, H.M. Volcanic arcs fed by rapid pulsed fluid flow through subducting slabs. *Nat. Geosci.* **2012**, *5*, 489–492. [CrossRef]

76. Lü, Z.; Zhang, L.F. Differential evolution of high-pressure and ultralhigh-pressure metapelites from Habutengsu, Chinese western Tianshan: Phase equilibria modelling and $^{40}Ar/^{39}Ar$ geochronology. *Acta Geol. Sin.* **2016**, *90*, 628–640.
77. Soldner, J.; Oliot, E.; Schulmann, K.; Štípská, P.; Kusbach, V.; Anczkiewicz, R. Metamorphic P–T–t–d evolution of (U)HP metabasites from the South Tianshan accretionary complex (NW China)—Implications for rock deformation during exhumation in a subduction channel. *Gondwana Res.* **2017**, *47*, 161–187. [CrossRef]
78. Wang, B.; Faure, M.; Shu, L.S.; Jong, K.; Charvet, J.; Cluzel, D.; Jahn, B.; Chen, Y.; Ruffet, G. Structural and geochronological study of high-pressure metamorphic rocks in the Kekesu section (Northwestern China): Implications for the late Paleozoic tectonics of the southern Tianshan. *J. Geol.* **2010**, *118*, 59–77. [CrossRef]
79. Zhang, L.F.; Ai, Y.; Li, X.; Rubatto, D.; Song, B.; Williams, S.; Song, S.; Ellis, D.; Liou, J.G. Triassic collision of western Tianshan orogenic belt, China: Evidences from SHRIMP U–Pb dating of zircon from HP/UHP eclogitic rocks. *Lithos* **2007**, *96*, 266–280. [CrossRef]
80. Zhang, L.F.; Du, J.X.; Shen, X.J. The timing of UHP–HP eclogitic rocks in Western Tianshan, NW China: The new SIMS U–Pb zircon dating, Lu/Hf and Sm/Nd isochron ages. In Proceedings of the 8th International Eclogite Conference, Xining, China, 25 August–3 September 2009; p. 177.
81. Liu, X.; Su, W.; Gao, J.; Li, J.; Jiang, T.; Zhang, X.; Ge, X. Paleozoic subduction erosion involving accretionary wedge sediments in the South Tianshan Orogen: Evidence from geochronological and geochemical studies on eclogites and their host metasediments. *Lithos* **2014**, *210*, 89–110. [CrossRef]
82. Du, J.X.; Zhang, L.F.; Shen, X.J.; Thomas, B. A new P–T–t path of eclogites from Chinese southwestern Tianshan: Constraints from P–T pseudosections and Sm–Nd isochron dating. *Lithos* **2014**, *200*, 258–272. [CrossRef]
83. Xia, B.; Zhang, L.F.; Thomas, B.; Shen, T.T.; Chen, N.S. Late Palaeozoic $^{40}Ar/^{39}Ar$ ages of the HP–LT metamorphic rocks from the Kekesu Valley, Chinese southwestern Tianshan: New constraints on exhumation tectonics. *Int. Geol. Rev.* **2016**, *58*, 389–404. [CrossRef]
84. Shen, T.T.; Wu, F.Y.; Zhang, L.F.; Hermann, J.; Li, X.P.; Du, J.X. In-situ U–Pb dating and Nd isotopic analysis of perovskite from a rodingite blackwall associatedwith UHP serpentinite fromsouthwestern Tianshan, China. *Chem. Geol.* **2016**, *431*, 67–82. [CrossRef]
85. Tan, Z.; Agard, P.; Gao, J.; John, T.; Li, J.L.; Jiang, T.; Bayet, L.; Wang, X.S.; Zhang, X. P–T–time-isotopic evolution of coesite-bearing eclogites: Implications for exhumation processes in SW Tianshan. *Lithos* **2017**, *278*, 1–25. [CrossRef]
86. Li, J.L.; Gao, J.; Wang, X.S. A subduction channel model for exhumation of oceanic-type high-pressure to ultrahigh-pressure eclogite-facies metamorphic rocks in SW Tianshan, China. *Sci. China Earth Sci.* **2016**, *59*, 2339–2354. [CrossRef]
87. Li, J.L.; Klemd, R.; Gao, J.; John, T. Poly-cyclic metamorphic evolution of eclogite: Evidence for multistage burial-exhumation cycling in a subduction channel. *J. Petrol.* **2016**, *57*, 119–146. [CrossRef]
88. Huang, D.Z.; Gao, J.; Zhang, J.F.; Zhang, D.X.; Dai, T.G.; Klemd, R. Study on oxygen isotope of high-pressure veins and host-rocks from southwestern Tianshan in China: Implications for deep fluids flow and the characteristic of subduction. *Acta Petrol. Sin.* **2006**, *22*, 74–82. (In Chinese with English Abstract)
89. Xiong, X.M.; Gao, J.; Klemd, R.; Huang, D.Z. Composition of hydrous fluids released by dehydration of oceanic island basalts during subduction: Constraints from the eclogite-facies high-pressure veins in the southwestern Tianshan, NW China. *Acta Petrol. Sin.* **2006**, *22*, 103–114. (In Chinese with English Abstract)
90. Xiong, X.M.; John, T.; Gao, J.; Klemd, R.; Huang, D.Z. Trace element mobilization in subducted slabs: Constraints on an eclogite facies transport vein from the southwestern Tianshan, NW China. *Acta Geol. Sin.* **2006**, *80*, 53–60. (In Chinese with English Abstract)
91. Zong, K.Q.; Liu, Y.S.; Hu, Z.C.; Kusky, T.; Wang, D.B.; Gao, C.G.; Gao, S.; Wang, J.Q. Melting-induced fluid flow during exhumation of gneisses of the Sulu ultrahigh pressure terrane. *Lithos* **2010**, *120*, 490–510. [CrossRef]
92. Liu, X.C.; Wu, Y.B.; Gao, S.; Wang, H.; Zheng, J.P.; Hu, Z.C.; Zhou, L.; Yang, S.H. Record of multiple stage channelized fluid and melt activities in deeply subducted slab from zircon U–Pb age and Hf–O isotope compositions. *Geochim. Cosmochim. Acta* **2014**, *144*, 1–24. [CrossRef]
93. Han, B.F.; He, G.Q.; Wang, X.C.; Guo, Z.J. Late Carboniferous collision between the Tarim and Kazakhstan–Yili terranes in the western segment of the South Tian Shan Orogen, Central Asia, and implications for the Northern Xinjiang, western China. *Earth Sci. Rev.* **2011**, *109*, 74–93. [CrossRef]

94. Xia, B.; Zhang, L.F.; Bader, T. Zircon U–Pb ages and Hf isotopic analyses of migmatite from the 'paired metamorphic belt' in Chinese SW Tianshan: Constraints on partial melting associated with orogeny. *Lithos* **2014**, *192*, 158–179. [CrossRef]
95. Xia, B.; Zhang, L.F.; Xia, Y.; Bader, T. The tectonic evolution of the Tianshan Orogenic Belt: Evidence from U–Pb dating of detrital zircons from the Chinese southwestern Tianshan accretionary mélange. *Gondwana Res.* **2014**, *25*, 1627–1643. [CrossRef]
96. Zhang, L.; Zhang, L.F.; Zhu, J.J.; Xia, B.; Lü, Z.; Thomas, B. Petrological Investigations and Zircon U–Pb Dating of High Pressure Felsic Granulites from the Yushugou Complex, South Tianshan, China. *Acta Geol. Sin.* **2018**, *92*, 144–161. [CrossRef]
97. Zhang, L.; Zhang, L.F.; Xia, B.; Lü, Z. Metamorphic P–T path and zircon U–Pb dating of HP mafic granulites in the Yushugou granulite–peridotite complex, Chinese South Tianshan, NW China. *J. Asian Earth Sci.* **2018**, *153*, 346–364. [CrossRef]
98. Bao, Z.H.; Cai, K.D.; Sun, M.; Xiao, W.J.; Wan, B.; Wang, Y.N.; Wang, X.S.; Xia, X.P. Continental crust melting induced by subduction initiation of the South Tianshan Ocean: Insight from the Latest Devonian granitic magmatism in the southern Yili Block, NW China. *J. Asian Earth Sci.* **2018**, *153*, 100–117. [CrossRef]
99. Gou, L.L.; Zhang, L.F.; Tao, R.B.; Du, J.X. A geochemical study of syn-subduction and post-collisional granitoids at Muzhaerte River in the Southwest Tianshan UHP belt, NW China. *Lithos* **2012**, *136*, 201–224. [CrossRef]
100. Xia, B.; Zhang, L.F.; Zhang, L. Petrogenesis and tectonic implications of Permian post-collisional granitoids in the Chinese southwestern Tianshan, NW China. *J. Asian Earth Sci.* **2016**, *130*, 60–74. [CrossRef]
101. Ren, R.; Han, B.F.; Ji, J.Q.; Zhang, L.; Xu, Z.; Su, L. U–Pb age of detrital zircons from the Tekes River 2016, Xinjiang, China, and implications for tectonomagmatic evolution of the South Tianshan Orogen. *Gondwana Res.* **2011**, *19*, 460–470. [CrossRef]
102. Ren, R.; Guan, S.W.; Han, B.F.; Su, L. Chronological constraints on the tectonic evolution of the Chinese Tianshan Orogen through detrital zircons from modern and palaeo-river sands. *Int. Geol. Rev.* **2017**, *59*, 1657–1676. [CrossRef]
103. Chen, R.X.; Zheng, Y.F.; Xie, L.W. Metamorphic growth and recrystallization of zircon: Distinction by simultaneous in-situ analyses of trace elements, U–Th–Pb and Lu–Hf isotopes in zircon from eclogite-facies rocks in the Sulu orogen. *Lithos* **2010**, *114*, 132–154. [CrossRef]
104. Hermann, J.; Rubatto, D.; Korsakov, A. Multiple zircon growth during fast exhumation of diamondiferous, deeply subducted continental crust (Kokchetav Massif, Kazakhstan). *Contrib. Mineral. Petrol.* **2001**, *141*, 66–82. [CrossRef]
105. Rubatto, D. Zircon trace element geochemistry: Partitioning with garnet and the link between U–Pb ages and metamorphism. *Chem. Geol.* **2002**, *184*, 123–138. [CrossRef]
106. Floyd, P.A.; Winchester, J.A. Identification and discrimination of altered and metamorphosed volcanic rocks using immobile elements. *Chem. Geol.* **1978**, *21*, 291–306. [CrossRef]
107. Corfu, F.; Davis, D.W. Comment on "Archean hydrothermal zircon in the Abitibi Greenstone Belt: Constraints on the timing of gold mineralization" by J.C. Claoué-Long, R.W. King and R. Kerrich. *Earth Planet. Sci. Lett.* **1991**, *104*, 545–552. [CrossRef]
108. Xia, Q.X.; Zheng, Y.F.; Hu, Z.C. Trace elements in zircon and coexisting minerals from low-T/UHP metagranite in the Dabie orogen: Implications for action of supercritical fluid during continental subduction-zone metamorphism. *Lithos* **2010**, *114*, 385–412. [CrossRef]
109. Rapp, J.F.; Klemme, S.; Butler, I.B.; Harley, S.L. Extremely high solubility of rutile in chloride and fluoride-bearing metamorphic fluids: An experimental investigation. *Geology* **2010**, *38*, 323–326. [CrossRef]